

Nonlinear wavepacket interferometry for polyatomic molecules

Jeffrey A. Cina^{a)}

Department of Chemistry and Oregon Center for Optics, University of Oregon, Eugene, Oregon 97403

(Received 10 July 2000; accepted 5 September 2000)

We investigate the application of a previously considered nonlinear wavepacket interferometry scheme to molecules with a single stable conformation in the electronic ground state. It is shown that interference experiments with pairs of phase-locked ultrashort pulse-pairs can be used to determine the complex overlaps of a nonstationary nuclear wavefunction evolving in an excited electronic state with a collection of compact displaced wavepackets moving in specified ways in the ground-state potential. © 2000 American Institute of Physics. [S0021-9606(00)00145-8]

I. BACKGROUND

It is a basic notion in quantum mechanics that the wavefunction of a system can be expressed as a linear superposition of any complete set of states, with the coefficients in the superposition being given by the complex overlaps between the state in question and each of the basis states. But opportunities to spectroscopically determine a set of overlaps characterizing a time-evolving molecular wavefunction are rare. We showed earlier that ultrafast fluorescence excitation experiments with a pair of electronically resonant phase-locked pulses¹ can be interpreted as providing the complex overlap between an evolving nuclear wavepacket in an excited electronic state and *one* reference state: the ro-vibrational eigenstate in the electronic ground state from which it originated.^{2,3} The signal in those linear optical experiments thereby directly revealed the time-dependent kernel for the electronic absorption spectrum.^{4,5} To specify the nuclear state completely, one would need to find its overlaps with a full manifold of vibrational wavefunctions.

With that goal in mind, in this paper we further investigate an experimental scenario for nonlinear optical measurements with *pairs* of phase-locked pulse pairs. Nonlinear wavepacket interferometry with pairs of pulse pairs was previously analyzed as a means to prepare and measure superpositions of nuclear wavefunctions corresponding to differently handed states of a chiral molecule.^{6,7} Here we consider the effects of similar measurements on molecules with a single stable conformation in the electronic ground state. Our interpretation in terms of interference between quantum mechanical wavepackets will be most natural for polyatomic molecules with several Franck–Condon active modes, at low temperature in a supersonic jet or in a cryogenic solid, but it could also apply in some approximation for the intramolecular modes of chromophores in solution. It is shown that wavepacket interferometry with pairs of pulse-pairs can yield the overlaps of an evolving wavepacket in a polyatomic molecule with a large set of wavepackets of specified mode displacements and momenta. In the limiting case of short excited-state propagation (briefer than all the mode periods) and some other specific situations, the overlaps comprise

those with a convenient set of nuclear wavefunctions akin to the Glauber coherent states.⁸ A surprising feature is that several signal contributions competing with the relevant overlaps are predicted to be small in many instances, are readily diminished with “averaging” sequences of related measurements, or else occur at distinguishable interpulse-pair delay times.

The advantage of nonlinear over linear wavepacket interferometry is the greatly expanded range of complex overlaps recorded by the interference signal. For fairly short excited-state propagation times (and some other particular cases) experiments of this kind can be sensitive to complex overlaps sufficient to specify completely a nuclear wavefunction in the chemically important region energetically “downhill” from the Franck–Condon point.

Time-resolved wavepacket interferometry posts an objective for molecular spectroscopy beyond the important missions of structure determination⁹ and the study of dynamics through the time development of probability densities,^{10,11} and also specifies a means to achieve it. The measured quantity in a wavepacket interferometry experiment is proportional to a targeted portion of the time-dependent wavefunction itself, rather than to its corresponding probability density. In the simple form proposed here and in a variety of possible generalizations, interference spectroscopy with sequences of phase-related pulses would use structural and dynamical information in one quantum mechanical subspace (a complete set of nuclear states in the electronic ground state for instance) to directly assay state development in other manifolds (electronic excited states). Iterative adjustment of molecular constants (defining excited-state potentials) would be avoided.

The objective of quantum state determination has been sought previously in atomic physics and quantum optics,¹² mostly in effectively one- or two-dimensional systems. The early work in this direction on the measurement of the density matrix of a light mode by optical homodyne tomography,^{13,14} is perhaps most closely related on a conceptual level. Recent experiments¹⁵ have determined the amplitude and phase of atomic Rydberg wavepackets by spectrally resolved cross correlation. Dunn, Walmsley, and Mukamel¹⁶ proposed and implemented an indirect method for state determination of a diatomic molecule using time-dependent

^{a)}Electronic mail: cina@oregon.uoregon.edu

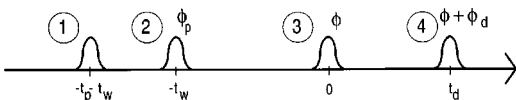


FIG. 1. The pulse sequence for nonlinear wavepacket interferometry with pairs of phase-locked pulse pairs. Pulses 1 and 2 are colinear and have an optical phase shift ϕ_p at the locking frequency Ω_p . Pulses 3 and 4 are colinear with phase shift ϕ_d at locking frequency Ω_d . 3 and 4 need not propagate colinearly with 1 and 2; there is an arbitrary phase shift ϕ between 2 and 3.

fluorescence¹⁷ as an approximate measure of vibrational probability density.

As we discuss later, interference spectroscopy with pairs of phase-locked pulse pairs has recently been proposed and implemented as a probe of chromophore solvation dynamics and optical dephasing of in liquids.^{18–20} Because both the molecular environment and the formal descriptions are different, the similarity to nonlinear wavepacket interferometry may not have been previously appreciated; but the successful execution of those “heterodyne-detected stimulated photon echo” experiments¹⁹ bodes well for speedy progress toward measurements of the kind proposed here.

II. BASIC IDEAS

The time-dependent Hamiltonian has a molecular part,

$$H = |g\rangle H_g \langle g| + |e\rangle H_e \langle e|, \quad (1)$$

involving the nuclear Hamiltonians in the ground and excited electronic states, and interactions $V(t) = V_1(t) + V_2(t) + V_3(t) + V_4(t)$ with four pulses for which

$$V_j(t) = -\mu(|e\rangle \langle g| + |g\rangle \langle e|) A_j(t-t_j) \times \cos[\Omega \cdot (t-t_j) + \Phi_j(t-t_j)]. \quad (2)$$

The transition dipole moment μ is assumed to be nuclear coordinate independent. All four pulses have the same carrier frequency, Ω , near the $e \leftarrow g$ absorption maximum. Their amplitudes $A_j(t)$ and phase functions $\Phi_j(t)$ will be specified later; but we assume that the pulses are vibrationally abrupt and that the delays $t_p = t_2 - t_1$, $t_w = t_3 - t_2$, and $t_d = t_4 - t_3$, while possibly short, are long enough that the pulses do not overlap (see Fig. 1).

The measured quantity is the “interference contribution” to the excited-state population proportional to $A_1 A_2 A_3 A_4$, which can be isolated within the total fluorescence (or another measure of excited-state population) as the portion dependent on all four field amplitudes.^{1,2} The e -state amplitude resulting from the four-pulse sequence can be determined by low-order time-dependent perturbation theory. Before the first pulse the molecule is in a nuclear eigenstate $|\psi_g\rangle$ in the electronic ground state $|g\rangle$. We choose the phase so that $|\Psi(t_0)\rangle = \exp[-iHt_0]|g\rangle|\psi_g\rangle$ and take $\hbar = 1$ to streamline the notation. The Schrödinger equation takes the form

$$i \frac{d}{dt} |\tilde{\Psi}(t)\rangle = \tilde{V}(t) |\tilde{\Psi}(t)\rangle, \quad (3)$$

in the interaction picture (related to the Schrödinger picture by $|\tilde{\Psi}(t)\rangle \equiv \exp[iHt]|\Psi(t)\rangle$ with $|\tilde{\Psi}(t_0)\rangle = |g\rangle|\psi_g\rangle$ initially).

The interaction-picture Hamiltonian, $\tilde{V}(t) \equiv e^{iHt} V(t) e^{-iHt} = \tilde{V}_1(t) + \tilde{V}_2(t) + \tilde{V}_3(t) + \tilde{V}_4(t)$, “turns on” only during the pulses. We need a perturbative solution of Eq. (3) through first order in each of the \tilde{V}_j 's, namely,

$$|\tilde{\Psi}(t)\rangle = \left(1 - i \int_{-\infty}^{\infty} d\tau_4 \tilde{V}_4(\tau_4)\right) \left(1 - i \int_{-\infty}^{\infty} d\tau_3 \tilde{V}_3(\tau_3)\right) \times \left(1 - i \int_{-\infty}^{\infty} d\tau_2 \tilde{V}_2(\tau_2)\right) \times \left(1 - i \int_{-\infty}^{\infty} d\tau_1 \tilde{V}_1(\tau_1)\right) |\tilde{\Psi}(t_0)\rangle. \quad (4)$$

At this point we make a rotating-wave approximation,^{21,22} which neglects rapidly oscillating and hence ineffectual terms in the integrands, by writing

$$\tilde{V}_j(t) \equiv -\frac{\mu A_j(t-t_j)}{2} |e\rangle \times \langle g| e^{-i\Omega \cdot (t-t_j) - i\Phi_j(t-t_j)} e^{iH_e t} e^{-iH_g t} + \text{H.c.} \quad (5)$$

It also proves useful to introduce *pulse propagators*,^{23–25} which reduce the effect of each pulse to the instantaneous action of an operator,

$$P_j = -\frac{\mu}{2} \int_{-\infty}^{\infty} d\tau A_j(\tau) e^{iH_e \tau} e^{-i(H_g + \Omega)\tau} e^{-i\Phi_j(\tau)}, \quad (6)$$

or its Hermitian conjugate. In Eq. (4) we can then recognize

$$\int_{-\infty}^{\infty} d\tau \tilde{V}_j(\tau) = |e\rangle \langle g| e^{iH_e t_j} P_j e^{-iH_g t_j} + \text{H.c.} \quad (7)$$

From its role in this expression, P_j is seen to govern the nuclear state-change accompanying electronic absorption, while P_j^\dagger effects the nuclear state-change during stimulated emission.

Odd numbers of E -field interactions generate transitions from the ground to the excited state, so the net transition amplitude predicted by Eq. (4) is a linear combination of eight nuclear wavepackets, with each term involving either one or three pulse propagators:

$$e^{-iH_e t_d} \langle e | \tilde{\Psi}(t > t_d) \rangle = \{U_A + U_B + U_C + U_D + T_A + T_B + T_C + T_D\} \times e^{iH_g(t_w + t_p)} |\psi_g\rangle. \quad (8)$$

The one-pulse contributions to (8) are specified by

$$U_A = -i \exp\{-iH_e(t_d + t_w + t_p)\} P_1, \quad (9a)$$

$$U_B = -i \exp\{-iH_e(t_d + t_w)\} P_2 \exp\{-iH_g t_p\}, \quad (9b)$$

$$U_C = -i \exp\{-iH_e t_d\} P_3 \exp\{-iH_g(t_w + t_p)\}, \quad (9c)$$

$$U_D = -i P_4 \exp\{-iH_g(t_d + t_w + t_p)\}, \quad (9d)$$

and the three-pulse wavepackets are generated by

$$T_A = i P_4 \exp\{-iH_g t_d\} P_3^\dagger \times \exp\{-iH_e t_w\} P_2 \exp\{-iH_g t_p\}, \quad (10a)$$

$$T_B = iP_4 \exp\{-iH_g t_d\} P_3^\dagger \exp\{-iH_e(t_w + t_p)\} P_1, \quad (10b)$$

$$T_C = iP_4 \exp\{-iH_g(t_d + t_w)\} P_2^\dagger \exp\{-iH_e t_p\} P_1, \quad (10c)$$

$$T_D = i \exp\{-iH_e t_d\} P_3 \exp\{-iH_g t_w\} P_2^\dagger \times \exp\{-iH_e t_p\} P_1. \quad (10d)$$

The various one-pulse and three-pulse wavepackets are illustrated schematically in Fig. 2.

The interference signal consists of the terms in $\langle \tilde{\Psi} | e \rangle \times \langle e | \tilde{\Psi} \rangle$ proportional to all four fields:

$$S_{\text{int}}(t_d) = 2 \text{Re} \langle \psi_g | T_A^\dagger U_A + T_B^\dagger U_B + T_C^\dagger U_C + T_D^\dagger U_D | \psi_g \rangle. \quad (11)$$

We have used the fact that $|\psi_g\rangle$ is an eigenket of H_g , and emphasized the t_d -dependence of the interference signal. Mixed combinations like $T_A^\dagger U_B$ contribute to the e -state population, but do not influence the signal because they exclude one of the pulses.

III. WAVEPACKET INTERFEROMETRY

The eight wavepackets in Fig. 2 follow different routes from the g -state to the e -state. The four terms in $S_{\text{int}}(t_d)$ are overlaps between these wavepackets, but for arbitrary delays, phase shifts, and pulse shapes, only the sum of the overlaps in Eq. (11) is measured. By considering basic features of how the nuclear wavefunctions evolve, we can nonetheless identify circumstances—and combinations of signals under different circumstances—where simultaneous contributions by more than one overlap are systematically avoided.

As mentioned earlier, a pulse propagator P_j applied to a nuclear wavepacket or eigenfunction on the ground potential surface generates the distorted “copy” which the j th pulse produces in the electronic excited state. Similarly, P_k^\dagger applied to an e -state wavepacket makes a distorted copy in the g -state. The distortions are less pronounced for shorter pulses, and a pulse briefer than the timescale for discernible nuclear motion (\sim inverse frequency width of the absorption spectrum) would make a copy identical to the original wavepacket (P_j reduces to a constant).

As Fig. 2 illustrates, the A -term in $S_{\text{int}}(t_d)$ is the real part of the overlap of $P_1|\psi_g\rangle$, prepared in the e -state by the first pulse and propagated for $t_p + t_w + t_d$, with a wavepacket copied to the e -state by P_2 and propagated for t_w , dumped back to g by P_3^\dagger and propagated for t_d , and finally, re-excited by P_4 . We will be interested in situations where the waiting time t_w is relatively long, while both the preparation time t_p and the delay time t_d will typically be relatively short (in senses to be specified later). In both wavefunctions overlapped in the A -term, the waiting-time evolution occurs in the excited electronic state. In a polyatomic molecule with several optically active vibrations, long-time e -state evolution will place most of the propagated wavepacket amplitude well away from the Franck–Condon region, with coordinate

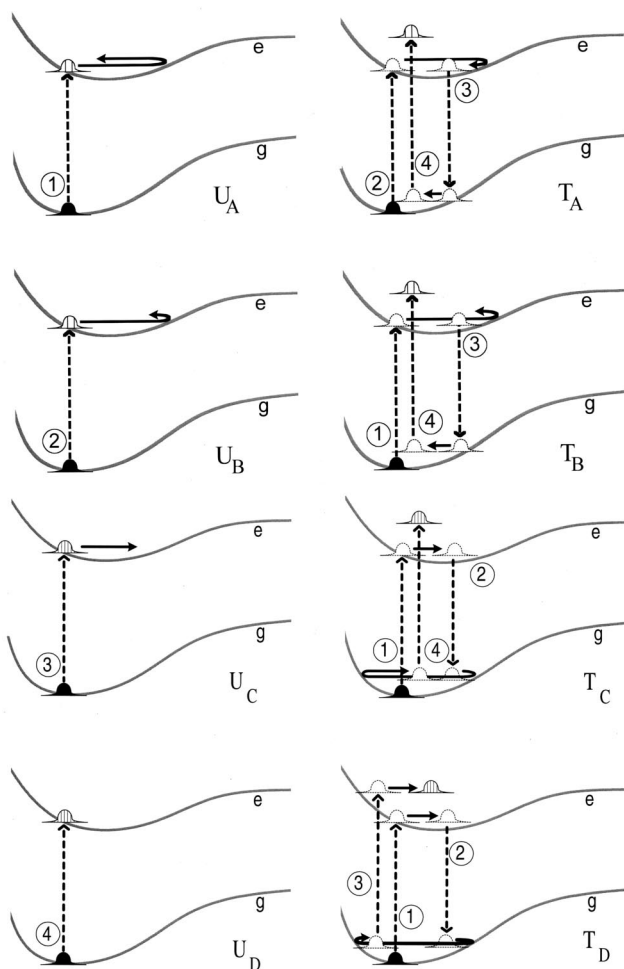


FIG. 2. One-pulse and three-pulse contributions to the nuclear wavefunction in the excited electronic state. See Eq. (8). The wavepacket interferometry signal (11) is a sum of overlaps of one-pulse and three-pulse wavepackets.

values for which the energetic spacing between the ground and excited-state electronic potential surfaces is red-shifted from the absorption maximum. Large-amplitude motion will also tend to bring anharmonicity into play, further disfavoring revisitation of the Franck–Condon region. The finite spectral bandwidth of pulses 3 and 4 (corresponding to their nonzero duration) will only inefficiently transfer nuclear amplitude between e and g at the nuclear configurations necessary to make $T_A|\psi_g\rangle$ sizable, and the A -term will tend to make a relatively small contribution to the interference signal.

The waiting-time evolution also occurs in the excited state for both wavepackets overlapped in the B -term. Bandwidth arguments again suggest that with pulses 3 and 4 centered at the absorption maximum, $T_B|\psi_g\rangle$ will be small for long t_w in a polyatomic molecule, so the B -term overlap will make little contribution to the interference signal.

Now let us consider the C -term portion of the interference signal. As shown in Fig. 2, it is the overlap between a one-pulse wavepacket ($P_3|\psi_g\rangle$) prepared by the third pulse and let run for t_d in the e -state) and a three-pulse wavepacket ($P_1|\psi_g\rangle$) prepared in the e -state by the first pulse and propagated for t_p , de-excited by P_2^\dagger and propagated for $t_d + t_w$ in

the g -state, and re-excited by P_4). For our purposes, the C -term overlap is the most interesting part of the interference signal: For a given t_d and various (t_p, t_w) it represents the overlap of a generic e -state wavepacket, $U_C|\psi_g\rangle$, with an array of moving reference packets, $T_C|\psi_g\rangle$. Because t_d is short, the one-pulse packet will be exploring the e -potential just downhill from the Franck–Condon region, while the reference packet will have moved in the vicinity of the g -potential minimum (t_p is also short) but with some wide choice of mode displacements and momenta (t_w is long and variable).

The D -term is less useful for wavepacket dissection than the C -term. It reports on the overlap between a three-pulse wavepacket (excited by the first pulse, de-excited by the second, and re-excited by the third) with a one-pulse wavepacket generated at the Franck–Condon point by the fourth pulse. Detailed consideration will be given shortly to whether and when it can make a contribution to the signal similar in size to the C -term.

The overlaps C and D are between pairs of wavepackets that have both propagated on the g -state potential during the waiting time t_w (see Fig. 2). The wavepacket $P_1|\psi_g\rangle$ created by the first pulse is assumed to be fairly close to the Franck–Condon region when the second pulse dumps it to the ground state. Subsequent motion in the g -state during $t_w + t_d$ (or t_w) in T_C (or T_D) starts with small displacements and momenta acquired by the optically active modes and stays in the vicinity of the potential-energy minimum. Stimulated de-excitation by P_2^\dagger and re-excitation by P_4 (or P_3) will not be discriminated against by bandwidth effects in either of these reference states.²⁶ Nor does anharmonicity disfavor the C - and D -term overlaps as it does the A - and B -terms.

Since the intramolecular g -state motion during $t_w + t_d$ (or t_w) in T_C (or T_D) involves small displacements and momenta, we may assume that it consists of nearly harmonic oscillations in the optically active modes. $T_C|\psi_g\rangle$ and $T_D|\psi_g\rangle$ will tend to “repeat themselves” whenever a near common multiple of the g -state periods of all the Franck–Condon modes is added to t_w . Multi-mode recurrences during the waiting-time are less likely for the larger-amplitude (hence less nearly harmonic) e -state trajectories of the A - and B -terms. And the period of any excited-state recurrence is unlikely to coincide with the period of g -state recurrences. This situation suggests a further—signal averaging—procedure for selectively enhancing interferences C and D over A and B : Signals of the same t_p and t_d , but with t_w differing by various multiples of the common g -state period, can be averaged together. This procedure would not affect the C and D interferences, but would systematically diminish the A - and B -term contributions.

IV. WAVEPACKET DECOMPOSITION

The interference signal of Eq. (11) is linearly proportional to the complex overlaps A – D themselves (rather than to the absolute square of their sum, for instance). To the extent that it proves possible to isolate the C -term experimentally, interference signals would yield some or all of the

inner products needed to resolve the excited-state wavepacket into a linear combination of reference states.

For the sake of further consideration, we assume that spectral discrimination, position-momentum space overlap effects, and t_w -averaging have effectively eliminated the A and B contributions to the interference signal. In the Appendix, we show that one way to produce C - and D -term signals while ensuring that the g -state motion occurs in the vicinity of the potential energy minimum is to choose roughly equal intrapulse-pair delays, $t_p \approx t_d \approx \delta t$, much shorter than the optically active mode periods. In this regime, the C -term and D -term contribute to the interference signal at distinctly different waiting times: $t_w(C) + \delta t \approx \tau_g^{\text{FC}}$ must approximately equal a common multiple of the g -state periods of the optically active modes, while $t_w(D) \leq h_g^{\text{FC}}$ must be just less than an approximate common odd multiple of all the half-periods (if such a time exists). (See the Appendix.) If we choose t_w when only the C -term contributes (or average several signals with such t_w values differing by close approximations to common multiples of the g -state periods) the interference signal (11) reduces to an overlap between the one-pulse wavepacket generated by U_C and the reference packet generated by T_C :

$$S_{\text{int}}(t_d) = 2 \text{Re}\langle \psi_g | T_C^\dagger U_C | \psi_g \rangle. \quad (12)$$

Let us look at the case where pulses 3 and 4 are transform-limited (i.e., unchirped) pulses with duration less than the inverse frequency-width of the absorption spectrum.²⁷ In this situation, the pulse propagators [see Eq. (6)] are given by²⁸

$$P_3 = -\mu E_3 s \sqrt{\frac{\pi}{2}} e^{-i\phi} \quad (13)$$

and

$$P_4 = -\mu E_4 s \sqrt{\frac{\pi}{2}} e^{-i(\phi + \phi_d + \Omega_d t_d)}. \quad (14)$$

Substituting these pulse propagators in Eqs. (9c), (10c), and (12), we get

$$S_{\text{int}}(t_d) = \pi \mu^2 E_3 E_4 s^2 \text{Re}\{\langle \alpha | \xi(t_d) \rangle e^{i\phi_d}\}. \quad (15)$$

For $\phi_d = 0$ (or $-\pi/2$) the interference signal therefore gives the real (or imaginary) part of the overlap between the original wavefunction propagated for t_d in the e -state,

$$|\xi(t_d)\rangle = \exp\{-iH_e t_d + i\Omega_d t_d\} \exp\{-iH_g(t_w + t_p)\} |\psi_g\rangle, \quad (16)$$

and a reference wavepacket specified by

$$|\alpha\rangle = -\exp\{-iH_g(t_d + t_w)\} P_2^\dagger \exp\{-iH_e t_p\} P_1 |\psi_g\rangle. \quad (17)$$

To the extent that various choices of t_p and t_w in the vicinity of the values maximizing the signal (15) provide an exhaustive set of states $|\alpha\rangle$ having significant overlap with $|\xi(t_d)\rangle$, the experiment would directly measure complex amplitudes sufficient to uniquely specify the nonstationary excited-state wavefunction.

V. REMARKS

Some examples can illustrate the C - and D -term interpulse-pair delay conditions identified in the Appendix. Methylene iodide has strongly Franck–Condon active low-frequency I–C–I vibrations with periods $\tau_g^{(ss)} = 66.8$ fs and $\tau_g^{(bend)} = 249$ fs.^{29,30} If we make the fairly stringent assumption that the quantity τ_g^{FC} in Eq. (A6) must be a common multiple of both periods within 10 fs we find C -term interferences at waiting times such that $t_w(C) + \delta t \approx 737, 1001, 1738, 2001$ fs (where both intrapulse-pair delays have small values of about δt). The condition (A7) for D -term interference predicts signals at waiting times $t_w(D) \leq 367, 632, 1106, 1369, 2107$ fs in CH_2I_2 . Spectral discrimination against the A and B overlaps should be very effective in this photodissociative system ($\lambda_{\text{peak}} \sim 312.5$ nm).²⁹ More definitive predictions will require wavepacket dynamical studies,³¹ but these estimates illustrate the conclusion of the Appendix that C - and D -term interference signals occur at different waiting times, t_w , in the case of short intrapulse-pair delay times.

The van der Waals molecule KrClF illustrates a case in which intrapulse-pair delays longer than a small fraction of the parent-molecule vibration could prepare g -state reference wavepackets in the vicinity of the potential minimum (see the Appendix).³² The van der Waals stretching mode of this molecule has a 765 fs period, while the vibrational period of ClF is 42.02 fs in the ground (X -) state and 91.8 fs in the B -state. If we choose $t_p \approx t_d \approx 91.8$ fs + $\delta t^{(\text{parent})} = \delta t^{(\text{vdW})}$, C -term overlaps would be expected when $t_w + t_d$ is an integer multiple of both 42.02 fs and 765 fs within several femtoseconds. By this argument—which assumes significant optical activity in the van der Waals stretch—signals are predicted near $t_w(C) + t_d = 760, 1520, \text{ and } 2300$ fs (as they would be for intrapulse-pair delays much shorter than both e -state periods). D -term signals for intrapulse-pair delays slightly longer than 91.8 fs are anticipated when the waiting time is just less than a half-odd multiple of both 42.02 fs and 765 fs. This criterion predicts signals at $t_w(D) \leq 390, 1150, 1912, 2670$ fs; and these waiting times differ from those for the C -signal as expected. The C -term signals for $t_p \approx t_d \approx 91.8$ fs – $\delta t^{(\text{parent})} = \delta t^{(\text{vdW})}$ just less than the e -state parent-stretching period occur at the same values of $t_w(C) + t_d$ (i.e., slightly longer waiting times). D -signals are now predicted at waiting times $t_w(D)$ just slightly longer than 390, 1150, 1912, 2670 fs.

In order to make better predictions of these nonlinear optical signals, we are carrying out wavepacket dynamical studies on various halogenated methane derivatives incorporating realistic pulse shapes and rotational structure.³³ It is anticipated that pulse chirp will be an effective tool to precompensate for wavepacket spreading during the preparation steps.^{34,24} Our prior studies of rotational effects in linear wavepacket interferometry on vapor phase samples^{2,35} suggest that rotational structure will not unduly complicate the interpretation at the ~ 10 K temperatures of supersonic jet spectroscopy experiments.

The nonlinear wavepacket interferometry scheme investigated here was originally proposed by Cina and Harris for the specific purpose of preparing and measuring quantum

mechanical superposition between nuclear states of a symmetric double-well like that governing the conformation of a chiral molecule.⁶ Wavepacket interferometry in this form would follow the approach of phase-locked linear absorption measurements demonstrated on vapor-phase I_2 by Scherer and co-workers, by measuring an interference contribution to the e -state population generated by an incident phase-locked pulse sequence. Rather than monitoring integrated fluorescence, or another direct measure of excited-state population, one could equally well monitor the interference contribution to transmission loss. In linear wavepacket interferometry, one would simply measure the E_1E_2 -contribution to sample-induced pulse-pair transmission loss.^{36,37} In nonlinear wavepacket interferometry, one would cross the preparation pulse-pair beam ($E_1 + E_2$) in the sample with the detection pulse-pair beam ($E_3 + E_4$), and measure the E_1E_2 “pump-interference” contribution to E_3E_4 “probe-interference” transmission loss. Just as linear wavepacket interferometry experiments are short-pulse absorption experiments with a fancy pulse (a phase-locked pulse-pair), nonlinear wavepacket interferometry experiments are pump–probe absorption experiments with pulse-pairs for both the pump and probe.

In addition to suggesting an experimental alternative to fluorescence excitation as a probe of nonlinear wavepacket interferometry, the last description also clarifies the essential similarity between the method proposed here and those known as “phase-locked pump–probe absorption”^{18,20} and “heterodyne-detected stimulated photon echoes.”^{18–20} In a phase-locked pump–probe experiment, a pump pulse-pair beam is to be crossed in the sample with a probe-pulse beam and a phase-locked “local oscillator” beam colinear and *contemporaneous* with the probe. This fits the description of our proposed experiments if the local oscillator is freed from simultaneity with the probe, and instead becomes the second sub-pulse in a probe pulse-pair. Recent heterodyne-detected stimulated photon echo experiments¹⁹ by de Boeij, Pschenichnikov, and Wiersma on solvation dynamics in liquids match this scenario almost exactly, but are of course subject to multi-mode effects, thermal averaging, and inhomogeneous broadening to a degree that would likely defeat a quantum mechanical wavepacket analysis. Wavepacket concepts have been of use in interpreting recent three-pulse four-wave mixing experiments on gas-phase species.³⁸ That work by Dantus and collaborators has many elements in common with the measurements proposed here.

The heterodyne-detected stimulated photon echo experiments¹⁹ yielded the system–bath correlation function governing chromophore transition-frequency fluctuations via numerical fits to the multimode Brownian oscillator model. In addition, their analysis^{18–20} demonstrated some capacity to separate the “echo” and “virtual echo” response functions. This capability of nonlinear phase-locked interference spectroscopy in liquids is reminiscent of linear wavepacket interferometry’s capacity to determine the portion of the time-dependent linear susceptibility involving a resonantly coupled electronic transition² and is also related in an inter-

esting way to wavepacket decomposition processes considered here.³⁹

It is interesting to contrast the source of the $t_p \approx t_d$ condition in a heterodyne-detected stimulated photon echo experiments and in the present theory. While quasi-static (inhomogeneous) broadening arising from weak optical activity in a large number of low frequency ($< kT$) degrees of freedom imposes this requirement on pl-HSPE signals, it emerges in nonlinear wavepacket interferometry as a nonexclusive dynamical condition for observable wavepacket overlap in a system with several strongly Franck–Condon active modes (the Appendix).⁴⁰ Moreover, the heterodyne-detected stimulated photon echo belongs to a class of ‘‘ideal’’ measurements whose simplest description accompanies the arbitrarily short-pulse limit.²⁰ In contrast, the use of spectral selection to diminish the *A*- and *B*-term interference signals in nonlinear wavepacket interferometry requires a finite spectral bandwidth.⁴¹

Superpositions of chiral amplitudes revisited. While the dynamical arguments in this paper have assumed a single stable conformation in the electronic ground state, the basic expression (11) for the interference signal should apply also to the double-well potential investigated by Cina and Harris.^{6,42} The interference signal given by the last two terms of Eq. (38) in Ref. 6 can be seen to correspond exactly to the *D*- and *C*-terms of Eq. (11) above. With the choice of t_p equal to the excited-state inversion time, those two terms are predicted to contribute simultaneously and with equal magnitudes. In the idealized model of a chiral molecule previously considered, ground state dynamics would not ensue for this value of t_p in the absence of tunneling. Spectral selection was used to eliminate the *A* and *B* overlaps in the double-well analysis, but it was justified by specializing to waiting times that placed the excited-state nuclear wavepackets directly above the ground-state potential barrier at the time of the third pulse.⁴³

The objection might be raised against wavepacket determination by nonlinear interferometry that preparation of the reference states involves motion (during t_p) on the very *e*-state potential surface where the target wavepacket evolves. This is not a fundamental feature of the method, however, but simply reflects our choice of a common center frequency for both preparation and detection pulse-pairs. If the center frequency of the preparation pulse-pair were chosen to access a well-characterized excited potential *e*-surface, and the detection pulse pair were resonant between the ground state and another (*f*) surface, the strategy proposed here would realize the ideal of wavepacket dissection within an external electronic *f*-subspace by experimental determination of overlaps with reference packets prepared in the subspace of *g*- and *e*-states. *No detailed information about the f-potential would be needed beforehand.* Nor is preparation restricted to a phase-locked stimulated Raman process. For instance, single-pulse resonant⁴⁴ or pre-resonant impulsive Raman excitation, or coherent infrared absorption could serve as well. If a means is available to control the optical phase shift between pulses of a different color, one could envisage a three-pulse version of nonlinear interferometry for wavefunction determination in which a reference wave-

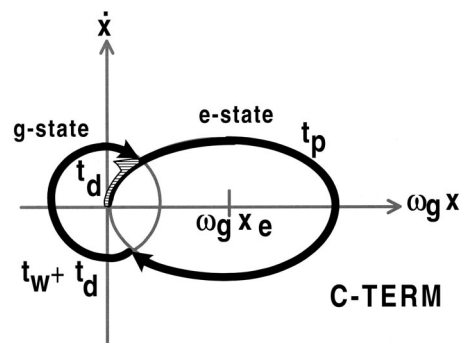


FIG. 3. A single mode phase-space diagram for the *C*-term interference signal. For a sizable overlap, a three-pulse reference packet (solid arrows) and one-pulse target (hatched arrow) must overlap in phase-space at the end of the pulse sequence.

packet is prepared in the *e*-state by resonant short-pulse excitation and a target packet in an *f*-state is interrogated with a final pulse of center frequency $\Omega_{fe} \cong \Omega_{fg} - \Omega_{eq}$.

ACKNOWLEDGMENTS

This paper is dedicated to Graham Fleming, at 50. I thank R. A. Harris and Chris Maierle for helpful conversations. Travis Humble prepared the figures. Victor Romero kindly shared some results from Ref. 43 in advance of their publication. The research was supported by a grant from the National Science Foundation.

APPENDIX: WHEN ARE INTERFERENCE SIGNALS C AND D NONZERO?

In order to gain a sense of when the *C*- and *D*-terms in the signal (11) will be most prominent, we investigate a simple case without mode mixing in the excited electronic state (no Duschinsky rotation). In this case, the system consists of an uncoupled collection of *g*- and *e*-state potential curves. The *g*-state can be assumed harmonic (see the main text) but the *e*-curves are displaced anharmonic oscillators. For the one-pulse and three-pulse wavepackets to overlap in the *C*- or *D*-term, the corresponding one-pulse and three-pulse classical trajectories starting from $(\omega_g x, \dot{x}) = (0, 0)$ for each mode (motionless at equilibrium in the ground state) must wind up near the same point in phase-space at time t_d .

For the *C*-term overlap to be sizable, motion for t_p in the *e*-state followed by motion for $t_d + t_w$ in the *g*-state must lead to the same phase-space point as motion for t_d in *e*. A single-mode trajectory of this type is shown in Fig. 3. In order that the *g*-state trajectory move in the vicinity of the potential minimum, t_p must not differ too greatly from an integer number of *e*-state vibrational periods, $\tau_e^{(a)}$, of mode *a*. Coincidence of the phase-points further requires that the two intrapulse-pair delays differ by similar amounts from integer $\tau_e^{(a)}$, so we need

$$t_p \approx k \tau_e^{(a)} + \sigma(\delta t^{(a)}) \quad \text{and} \quad t_d \approx l \tau_e^{(a)} + \nu(\delta t^{(a)}), \quad (\text{A1})$$

where *k* and *l* are non-negative integers, $\sigma, \nu = \pm 1$, and $\delta t^{(a)} (> 0)$ is much shorter than $\tau_e^{(a)}$. The four cases (A1) impose different conditions on the interval $t_w + t_d$:

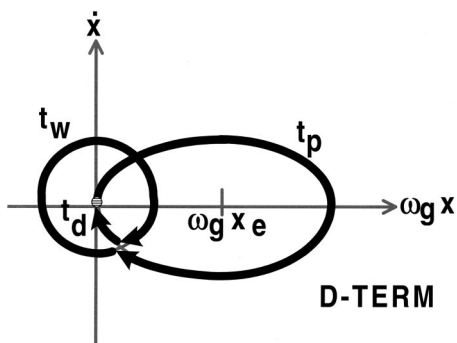


FIG. 4. The same as Fig. 3, but for a D -term signal. The one-pulse wavepacket is at the Franck–Condon point.

$$\begin{aligned}
 t_w + t_d &\approx m \tau_g^{(a)} & (\sigma, \nu) &= (1, 1); \\
 t_w + t_d &\geq (m + 1/2) \tau_g^{(a)} & (\sigma, \nu) &= (-1, 1) \quad (\text{illustrated}); \\
 t_w + t_d &\leq (m + 1/2) \tau_g^{(a)} & (\sigma, \nu) &= (1, -1); \\
 t_w + t_d &\approx m \tau_g^{(a)} & (\sigma, \nu) &= (-1, -1);
 \end{aligned} \tag{A2}$$

where $\tau_g^{(a)} (= 2\pi/\omega_g^{(a)})$ is the period in the electronic ground state and m is a non-negative integer.

Figure 4 illustrates one-pulse and three-pulse mode trajectories that lead to a D -term overlap. For this term to contribute to the signal, sequential motion for t_p in the e -state, t_w in the g -state, and t_d in the e -state must leave the mode motionless at the Franck–Condon point, so that $(\omega_g x, \dot{x}) \approx (0, 0)$ once again t_d after the end of the 1–2–3 pulse sequence. The four cases of intrapulse-pair delays (A1) lead to the following conditions on t_w :

$$\begin{aligned}
 t_w &\leq (n + 1/2) \tau_g^{(a)} & (\sigma, \nu) &= (1, 1); \\
 t_w &\approx n \tau_g^{(a)} & (\sigma, \nu) &= (-1, 1) \quad (\text{illustrated}); \\
 t_w &\approx n \tau_g^{(a)} & (\sigma, \nu) &= (1, -1); \\
 t_w &\geq (n + 1/2) \tau_g^{(a)} & (\sigma, \nu) &= (-1, -1);
 \end{aligned} \tag{A3}$$

where n is a non-negative integer.

Short intrapulse-pair delay case. One way to satisfy conditions (A1) simultaneously for several optically active modes with different periods is to choose $t_p \approx t_d \approx \delta t$ short enough so that the individual mode coordinates do not change greatly from their values in the Franck–Condon region. In this situation, $(\sigma, \nu) = (1, 1)$ for every mode. When both intrapulse-pair delays are short, there is a propensity for the C - and D -terms to give signals at different t_w values because the waiting-time choices,

$$t_w \approx \tau_g^{(a)} - \delta t, 2\tau_g^{(a)} - \delta t, 3\tau_g^{(a)} - \delta t, \text{ or } \dots, \tag{A4}$$

from Eq. (A2) and

$$t_w \leq \tau_g^{(a)}/2, 3\tau_g^{(a)}/2, 5\tau_g^{(a)}/2, \text{ or } \dots, \tag{A5}$$

from Eq. (A3) are incompatible for short δt . For a strongly Franck–Condon active mode, these t_w conditions will turn off the C -signal, the D -signal, or both.

Are there waiting times when either of these signals survives in a polyatomic molecule with several optically active modes of different frequencies? Equation (A4) for the C -term implies that the $t_w + \delta t$ episode of ground-state motion must be an integer multiple of all the mode periods. Nonzero C -term signals can only occur at waiting times,

$$t_w(C) \approx \tau_g^{\text{FC}} - \delta t, \tag{A6}$$

where τ_g^{FC} is a common multiple of all the mode periods to some adequate approximation that depends on the spatial and momentum width parameters of the wavepacket and on δt itself.

The multi-mode condition for the D -signal is different and more restrictive. To satisfy one of the choices (A5) for each of several optically active modes requires a waiting time just less than a common odd multiple all the half-periods:

$$t_w(D) \leq h_g^{\text{FC}}. \tag{A7}$$

Such common odd multiples h_g^{FC} do not exist for every molecule. If a certain period happens to be an even multiple of another vibration, for instance, then any odd multiple of the latter is still an even multiple of the former. τ_g^{FC} and h_g^{FC} do not coincide of course, so for short $t_p \approx t_d \approx \delta t$ and D -term interference signals that do materialize will tend to occur at different waiting times from the C -term signals.

Longer intrapulse-pair delay cases. If we let one or both of t_p and t_d take on longer values, any of the (σ, ν) combinations in Eqs. (A2) and (A3) can come into play. Different combinations may apply to different modes and these assignments could shift with small changes in the intervals t_p and t_d . Analysis becomes difficult without specifying the actual mode periods. Anharmonicity, intermode coupling, and wavepacket spreading cannot generally be ignored during long episodes of e -state evolution, so the assumptions of a trajectory-based analysis are unlikely to remain valid for long t_p or t_d .

There is one long intrapulse-pair delay case where direct computation may not be necessary. If the highest-frequency Franck–Condon active mode has an excited-state period $\tau_e^{(1)}$ several times shorter than the rest, we may choose $t_p \approx t_d \approx \tau_e^{(1)} + \sigma^{(1)} \delta t^{(1)}$ fairly close to a full e -state period and still have the intrapulse-pair delays much shorter than the other vibrational periods. With t_p and t_d at the solid vertical line in Fig. 5, $(\sigma^{(1)}, \nu^{(1)}) = (-1, -1)$ for the high-frequency mode, but $(\sigma^{(a)}, \nu^{(a)}) = (1, 1)$ for all others. If the intrapulse-pair delays are moved to the dashed vertical, then $(\sigma^{(a)}, \nu^{(a)}) = (1, 1)$ for all modes. Notice that one cannot freely separate the intrapulse-pair delays for this system. If t_p were kept at the

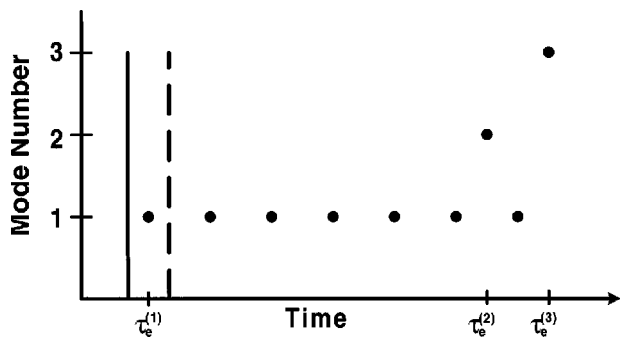


FIG. 5. A longer intrapulse-pair delay case for the system with one high-frequency mode, period $\tau_e^{(1)}$, and two lower-frequency modes. Shown are $t_p \approx t_d$ just less (solid vertical line) and just more (dashed) than $\tau_e^{(1)}$. See the text of the Appendix.

solid line and t_d moved to the dashed line, then $(\sigma^{(1)}, \nu^{(1)}) = (-1, 1)$ would apply to mode 1, but t_p and t_d may differ enough that phase-point coincidence is no longer possible for the other vibrations.

¹N. F. Scherer, A. J. Ruggiero, M. Du, and G. R. Fleming, *J. Chem. Phys.* **93**, 856 (1990); N. F. Scherer, R. J. Carlson, A. Matro, M. Du, A. J. Ruggiero, V. Romero-Rochin, J. A. Cina, G. R. Fleming, and S. A. Rice, *ibid.* **95**, 1487 (1991).

²N. F. Scherer, A. Matro, L. D. Ziegler, M. Du, R. J. Carlson, J. A. Cina, and G. R. Fleming, *J. Chem. Phys.* **96**, 4180 (1992).

³See also H. Metiu and V. Engel, *J. Opt. Soc. Am. B* **7**, 1709 (1990); R. Bavli, V. Engel, and H. Metiu, *J. Chem. Phys.* **96**, 2600 (1992).

⁴See E. J. Heller's chapter in *Advances in Classical Trajectory Methods*, edited by W. L. Hase (JAI Press, Greenwich, 1992), Vol. I, p. 165.

⁵See Secs. III.B, IV.D, and V of Ref. 2.

⁶J. A. Cina and R. A. Harris, *J. Chem. Phys.* **100**, 2531 (1994).

⁷J. A. Cina and R. A. Harris, *Science* **267**, 832 (1995).

⁸C. Cohen-Tannoudji, B. Diu, and F. Lalöc, *Quantum Mechanics* (Wiley, New York, 1977), Vol. I, Complement G_v .

⁹D. W. Pratt, *Annu. Rev. Phys. Chem.* **49**, 481 (1998).

¹⁰D. J. Tannor and S. A. Rice, *J. Chem. Phys.* **83**, 5013 (1985).

¹¹A. H. Zewail, *Science* **242**, 1645 (1988).

¹²D. Leibfried, T. Pfau, and C. Monroe, *Phys. Today* **1998**, 22, and references therein.

¹³D. T. Smithy, M. Beck, M. G. Raymer, and A. Faridani, *Phys. Rev. Lett.* **70**, 1244 (1993); K. Vogel and H. Risken, *Phys. Rev. A* **40**, 2847 (1989).

¹⁴M. G. Raymer, A. C. Funk, and D. F. McAlister, in *Quantum Communication, Computing, and Measurement 2*, edited by P. Kumar, G. Mauro D'Ariano, and O. Hirota (Kluwer Academic/Plenum, New York, 2000), p. 147.

¹⁵T. C. Weinacht, J. Ahn, and P. H. Bucksbaum, *Phys. Rev. Lett.* **80**, 5508 (1998).

¹⁶T. J. Dunn, I. A. Walmsley, and S. Mukamel, *Phys. Rev. Lett.* **74**, 884 (1995).

¹⁷L. W. Ungar and J. A. Cina, *Adv. Chem. Phys.* **100**, 171 (1997).

¹⁸M. Cho, N. F. Scherer, G. R. Fleming, and S. Mukamel, *J. Chem. Phys.* **96**, 5618 (1992).

¹⁹W. P. de Boeij, M. S. Pschenichnikov, and D. A. Wiersma, *Chem. Phys.* **233**, 287 (1998).

²⁰Shaul Mukamel's comprehensive book, *Principles of Nonlinear Optical Spectroscopy* (Oxford University Press, New York, 1995), gives theoretical treatments of a wide variety of nonlinear optical methods for molecular spectroscopy and details some of their added capabilities relative to linear measurements. Of particular relevance here are Chaps. 5, 10, and 11.

²¹If the pulses are so short (less than a few optical cycles) and the system dynamics so rapid (competitive with the electronic transition frequency) that the rotating wave approximation breaks down, one could turn to an alternative approach to electronic interference spectroscopy that has recently been developed; see A. W. Albrecht, J. D. Hybl, S. M. Gallagher Faeder, and D. M. Jonas, *J. Chem. Phys.* **111**, 10934 (1999). In that work

a method for *clocking* intrapulse-pair delays by spectral interferometry rather than controlling them, as in the original phase-locking scheme of Scherer and co-workers (Refs. 1 and 2), is demonstrated. This new technique can operate even when the undersampling rate, $(1/2\pi)\Omega_L$, of conventional phase locking is inadequate.

²²The rotating wave approximation—like the similarly motivated Born–Oppenheimer approximation—can be surprisingly resilient, however. In the theoretical studies of Ref. 23 we looked for but did not find significant deviations from the rotating wave approximation for pulses as short as 2.8 fs intensity-FWHM resonant with the $B \leftarrow X$ transition of I_2 .

²³Y.-C. Shen and J. A. Cina, *J. Chem. Phys.* **110**, 9793 (1999).

²⁴J. Cao and K. R. Wilson, *J. Chem. Phys.* **107**, 1441 (1997); J. Cao, J. Che, and K. R. Wilson, *J. Phys. Chem. A* **102**, 4284 (1998).

²⁵S. Dilthey, S. Hahn, and G. Stock, *J. Chem. Phys.* **112**, 4910 (2000).

²⁶The discrimination against the A- and B-term three-pulse reference packets relative to those of the C- and D-terms could be made to operate in the opposite way by shifting the carrier frequency for pulses 3 and 4 well to the red of the absorption maximum.

²⁷We should be aware, however, that this limit begins to militate against spectral elimination of the A- and B-term overlaps.

²⁸We use Gaussian envelopes $A_j(t) = E_j \exp(-t^2/2s^2)$ for pulses 3 and 4, where s is the pulse duration, and phase functions $\Phi_3 = \phi$ and $\Phi_4 = \phi + \phi_d + \Omega_d t_d$. ϕ_d is the relative optical phase between pulses 3 and 4 at the locking frequency Ω_d , and ϕ is an arbitrary overall phase for those two pulses, which does not affect the interference signal [see Eq. (2)].

²⁹W. M. Kwok and D. L. Phillips, *J. Chem. Phys.* **104**, 2529 (1996).

³⁰See also D. L. Phillips, *Prog. React. Kinet.* **24**, 223 (1999).

³¹J. Zhang, E. J. Heller, D. Huber, D. G. Imre, and D. J. Tannor, *J. Chem. Phys.* **89**, 3602 (1988).

³²S. E. Novick, S. J. Harris, K. C. Janda, and W. Klemperer, *Can. J. Phys.* **53**, 2007 (1975).

³³T. Humble and J. Cina (work in progress).

³⁴Shen and Cina (Ref. 23) recently obtained approximate closed-form expressions for the effect of frequency-chirp on the position and momentum moments of a short-pulse excited wavepacket that will be useful in shaping the preparation pulses.

³⁵V. Blanchet, M. A. Bouchène, and B. Girard, *J. Chem. Phys.* **108**, 4862 (1998).

³⁶Equations (3.8) and Eq. (3.13) of Ref. 2 give the interference contribution to photon absorption in terms of the vibronic transition energies and Franck–Condon factors; these equations would apply to either fluorescence excitation or transmission loss.

³⁷The essential equivalence of fluorescence excitation and transmission loss as measures of the interference contribution to photon absorption has been emphasized recently by Ref. 21. That paper is not entirely accurate in portraying the findings of Refs. 1 and 2, however. It ascribes to that work an assertion that phase-locked absorption experiments measure contributions to the optical free-induction decay from “nonresonant, virtually excited transitions with Bohr frequencies which may lie either inside or outside the pulse spectrum” (Ref. 21). But the existence of such contributions to the optical free induction decay induced by the first pulse in a linear wavepacket interferometry experiment is easily disproved, as only vibronic transitions within the pulse spectrum make persisting contributions to the pulse-induced dipole moment. Reference 2 emphasized that while in-phase and in-quadrature interference signals obtained with pulses short compared to the inverse absorption linewidth can be combined to yield the complete $e \leftarrow g$ linear response function [as in Eq. (3.16) of Ref. 2] this is not strictly possible for longer pulses: “If the laser pulses are not arbitrarily abrupt, one can no longer write down an expression relating $\chi(t_d)$ to the interference population; the finite spectral range of the pulses prohibits the complete determination of the system's response.” The claim inaccurately attributed to the original analysis would also contradict expressions (3.24) and (3.23) of paper 2 for the experimentally derived dispersive and absorptive susceptibility components, both of which contain pulse-envelope-modulated vibronic transition moments. That these two quantities are related by a (formally reciprocal) Kramers–Kronig transformation is evident from their parallel structure with the complete $e \leftarrow g$ susceptibilities [(3.20) and (3.19) or Ref. 2]. Each of the susceptibility components assembled from the measured phase-locked transients according to the prescriptions (3.24) and (3.23) has the same form as the corresponding component of the full susceptibility, but with envelope-modulated vibronic transition moments replacing the ordinary Franck–Condon factors.

- ³⁸I. Pastirk, E. J. Brown, B. I. Grimberg, V. V. Lozovoy, and M. Dantus, *Faraday Discuss.* **113**, 401 (1999); E. J. Brown, Q. Zhang, and M. Dantus, *J. Chem. Phys.* **110**, 5772 (1999); and I. Pastirk, V. V. Lozovoy, B. I. Grimberg, E. J. Brown, and M. Dantus, *J. Phys. Chem. A* **103**, 10226 (1999). The effects of pulse timing on homodyne-detected degenerate four-wave mixing signals—proportional to the square of the phase-matched component of the third-order induced polarization—are detailed by V. V. Lozovoy, I. Pastirk, E. J. Brown, B. I. Grimberg, and M. Dantus, *Int. Rev. Phys. Chem.* (in press).
- ³⁹The A – D overlaps in the present theory correspond in simple ways to the R_1 – R_4 nonlinear response functions, respectively, that contribute to the third-order polarization in Mukamel's analysis (Ref. 20). Despite the widespread application of this useful formalism, the possibility to spectrally select C - and D -type terms (corresponding to R_3 and R_4) over A - and B -terms (R_1 and R_2), or *vice versa*, does not seem to have been noted previously. But some spectral-selection arguments are made in Refs. 38 (see Fig. 5 of the last article listed, for example).
- ⁴⁰The arguments in the Appendix are reminiscent of conditions for vibrational mode suppression in photo-echo experiments identified by C. J. Bardeen and C. V. Shank, *Chem. Phys. Lett.* **203**, 535 (1993).
- ⁴¹It is worth noting, however, that if nonlinear wavepacket interferometry experiments were used to monitor excited-state intramolecular vibrational wavefunctions of solvated species, inhomogeneous broadening could help suppress the D - (and A -) terms relative to C (and B); see Chap. 10 of Ref. 20.
- ⁴²See also J. A. Cina and R. A. Harris, *Ultrafast Phenomena IX*, edited by W. Knox and P. Barbara (Springer-Verlag, Berlin, 1994), p. 486; C. S. Maierle and R. A. Harris, *J. Chem. Phys.* **109**, 3713 (1998). For an up-to-date survey of work addressing the preparation and measurement of molecular superposition states, see C. S. Maierle, Ph.D. dissertation, University of California at Berkeley, 1999.
- ⁴³Forthcoming numerical calculations by R. P. Duarte-Zamorano and V. Romero-Rochín explore the effects of nonzero pulse duration in the model of Ref. 6 and quantify the limits of validity of various approximations used in that study.
- ⁴⁴J.A. Cina, *J. Raman Spectrosc.* **31**, 95 (2000), and references therein.